URTeC: 604

NMR Wettability Index Measurements on Unconventional Samples

M.J. Dick[1], D. Veselinovic[1], D. Green[1], A. Scheffer-Villarreal[2], R. J. M. Bonnie[3], S. Kelly[3] and K. Bower[3]

[1]*Green Imaging Technologies, Fredericton, NB, Canada*

[2]*ConocoPhillips, Anchorage, AK*

[3]*ConocoPhillips, Houston, TX*

Abstract

Wettability is a crucial petrophysical parameter for determining accurate production rates in oil and gas reservoirs and may be especially impactful in predicting the extent of injected fluid imbibition and resultant drainage in the vicinity of hydraulic fractures within unconventional reservoirs. However, traditional industry standard wettability measurements (Amott test and USBM) often fall short when performed on unconventional samples. In this work, we adapt the existing T_2-based NMR wettability index (NWI) measurement to unconventional samples in order to provide robust wettability measurements for tight rocks.

Introduction

Wettability describes the affinity of a fluid to a solid surface and is dependent on rock properties such as mineralogy, aging, and brine and hydrocarbon composition. As a system always seeks to minimize surface energy toward equilibrium, whether a surface is hydrophobic (prefers to contact non-aqueous fluid molecules, usually of lesser polarity than water) or hydrophilic (prefers water) will determine the native state distribution of brine and hydrocarbon as well as the dynamic behavior of these saturations. It is well known in conventional reservoirs that wettability can greatly influence the character of relative permeability curves and production. Conventionally, water wet is the preferred state for petroleum exploration, as water will reside in the smallest pores and hydrocarbons in the larger pores and apertures, but many successful reservoirs have mixed (or intermediate) wettability. The tight pore structures of unconventional reservoirs are also sensitive to wettability controls, if not governed by them due to strong capillarity; however, the influence of wettability on matrix and matrix-fracture transport during and after hydraulic fracturing is not as well understood as in (or for?) conventional reservoirs. Learnings on the role

of wettability in unconventional rocks may render useful information for the design of well completion and enhanced oil recovery strategies.

A wettability assessment such as NWI may assist with testing wettability states and controls in tight rocks in a quantitative matter. Recall that a wettability index of 1 is very water wet, -1 is very oil wet, 0 is neutral/mixed wet, and values close to 0 are weakly oil or water wet. This research demonstrates the utilization of the NWI technique on two twin sets of South Texas unconventional core plugs expected to have differing wettability due to significantly higher organic matter content in one of the sample sets. The samples, generally labeled sample 2-PX and 7-PX, are from the same well in producing acreage, but different lithological units. Sample 2-PX is a chalk and sample 7-PX is a marl; the latter has significant organic matter and clay content. Some basic petrophysical properties of these samples are listed in Table 1.

Methods

It is known [1-7] that NMR response varies as a function of wettability changes in rock core plug samples. This information was used to develop an NMR wettability index (NWI) based on T_2 distributions [6-7]. The NWI method is capable of measuring changes in wettability as a function of oil/water saturations unlike traditional methods which are based on measurements at S_{wi} and S_{or} only. In order to derive an NMR wettability index, NMR T_2 spectra of (1) 100% brine saturated sample, (2) 100% oil (decane) saturated sample, (3) bulk oil and (4) bulk brine are needed. These spectra are then mixed to give a predicted T_2 spectrum which is compared (via a least-squares fit) to a T_2 spectrum recorded from a sample partially saturated with both water and oil whose wettability is to be determined. We have developed a new model which is an extension of the Looyestijn et. al. [6-7] technique and considers the dual porosity systems often found in shales, one associated with organics and the other being the intergranular network. As is often the case in unconventional reservoirs, these two networks may have different wetting-conditions. The model assumes that the organic network is oil wet and that crystalline networks are water wet. The wettability of the sample is a combination of wettability contributions from both pore networks.

Theory

Looyestijn [6-7] has already discussed the derivation of his NMR wettability analysis. We will instead only present an overview of how we implemented his wettability analysis in this work.

As shown in Equations 1 and 2, we employed the same functions derived by Looyestijn [6] to describe the saturation and wettability as a function of pore size.

$$H = \frac{a_1 - a_2}{1+\left(\frac{r}{r_a}\right)^{\alpha}} + a_2 \rightarrow \frac{1}{1+\left(\frac{T_2}{r_a}\right)^2}, W = \frac{b_1 - b_2}{1+\left(\frac{r}{r_b}\right)^{\beta}} + b_2 \rightarrow \frac{1}{1+\left(\frac{T_2}{r_b}\right)^2} \quad (1,2)$$

H describes the fraction of pores occupied by water and W describes the fraction of pores wetted by water. Following the work of Looyestijn [6] which found these constants to be the same for all rocks, we fixed a_1 and b_1 = 1, a_2 and b_2 equal to 0 as well as α and β equal to 2. We also substituted r by T_2 as transverse relaxation time is proportional to pore size. The typical form of these equations are plotted as the light blue (*H*) and pink lines (*W*) in Figure 1. These functions are like step functions, where for example, all pores to the left of the inflection point of the *W* function are wetted by water and all the pores

to the right of the inflection point of the *W* function are wetted by oil (decane). Conversely all the pores to the left of the inflection point of the *H* function are occupied by brine and all the pores to the right of the inflection point of the *H* function are occupied by decane. These functions act as mixing functions that combine the 100% oil (decane) saturated, 100% brine saturated, bulk brine and bulk decane T_2 distributions to give a simulated mixed saturation T_2 distribution which closely agrees with the measured mixed saturation T_2 distribution. How this mixing is carried out will now be explained.

All the wettability analysis was carried out in a Matlab routine which read in the T_2 distributions from GIT systems [8]. It should be noted that all our analysis was done in the spectral (T_2) domain. As mentioned by Looyestijn [6], fitting in the time domain is acceptable and sometimes preferred. However, we chose to fit in the spectral domain as we found the analysis was faster. We did however carry out a limited amount of analysis in the time domain and verified that the spectral analysis was consistent with the time domain analysis.

The first step in the wettability determination is to read in the bulk brine ($S_{w\text{-}bulk}$), bulk oil ($S_{o\text{-}bulk}$), 100% brine saturated ($S_{w\text{-}100\%}$), 100% oil saturated ($S_{o\text{-}100\%}$) and mixed wettability (S_{mix}) T_2 distributions into the wettability analysis program. Next, the area under each distribution was normalized. Figure 1 shows a plot of each of these normalized T_2 distributions. Next, a predicted mixed wettability T_2 distribution (S_{pred}) is generated according to Equation 3.

$$S_{pred} = WHS_{w-100\%} + (1-W)(1-H)S_{o-100\%} + (1-W)HS_{w-bulk} + W(1-H)S_{o-bulk} \quad (3)$$

How *W* and *H* act as mixing functions is now apparent. By multiplying the step functions by the measured T_2 distributions allows portions of each measured spectrum to be combined to give the predicted mixed wettability distribution. The positions of *W* and *H* can be adjusted by varying r_a and r_b in Equations 1 and 2 giving different contributions to the predicted distributions from each measured distribution. Specifically, a least-squares fit (varying only r_a and r_b) is carried out to minimize the difference between S_{mix} and S_{pred}. The black trace in Figure 1 shows the final predicted T_2 distribution generated from the final *H* (Figure 1 – light blue trace) and *W* (Figure 1 – pink trace) functions derived from the least squares fitting. As can be seen the final predicted spectrum agrees quite well with the measured mixed saturation distribution (Figure 1- brown trace).

Once the final *H* and *W* functions are known, the saturation and wettability can be quantitatively defined according to Equations 4 and 5. For the data shown in Figure 1, this corresponds to a Predicted Water Saturation (S_{wett}) = 0.13 and NMR Wettabililty Index (NWI) = 0.89.

$$Water\ Saturation = S_{wett} = \sum_{T_2} S_{w-100\%}H \quad (4)$$

$$Wettability = NWI = 2\sum_{T_2} S_{w-100\%}W - 1 \quad (5)$$

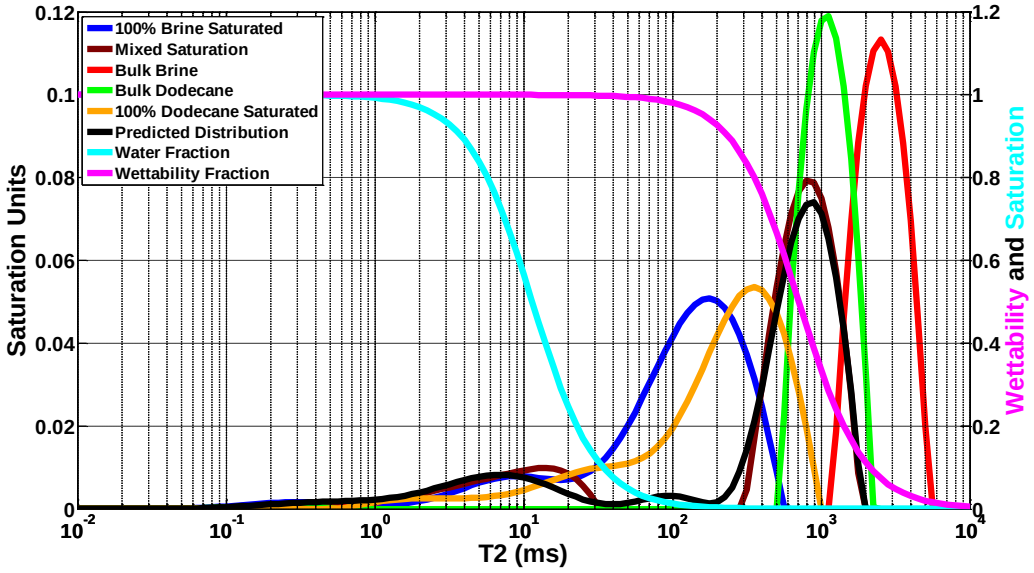

Figure 1: Typical bulk-T_2 spectra used for wettability determination (left axis). The water fraction (light blue) and wettability fraction (pink) are also shown (right axis). This data is for instructional purposes only was not recorded as part of this investigation of wettability of unconventional samples.

Experiment:

Two sets of twin unconventional rock core plugs from the same South Texas well, but different units, were used in this wettability study. The physical properties of these samples are summarized in Table 1. For each set of twins (Twins 1: 7-P2/7-P3A and Twins 2: 2-P2/2-P1A), one of the twins was brine (4% NaCl in water) saturated while the other one was decane saturated. See Table 1 to reference which twin was saturated by brine and which was saturated by decane. T_2 NMR spectra were acquired on each sample in these initial states, using an NMR instrument [9] and the data acquisition and analysis software [8]. Table 2 summarizes the NMR parameters employed. T_2 spectra for bulk brine and decane were also recorded. Table 2 also summarizes the NMR parameters employed for these scans.

The goal of this experiment was to observe wettability changes in the unconventional samples under study. To achieve changes in wettability, the decane saturated samples were submerged in brine while the brine saturated samples were submerged in decane. Spontaneous imbibition of each fluid/sample combination was monitored over time and T_2 distributions were acquired periodically during the imbibition process. Figure 2 shows water droplets forming on the surface of one of the 100% brine saturated shale samples after imbibition of decane. These T_2 spectra were then employed as the mixed wettability distributions (S_{mix}) and were fit along with the bulk brine ($S_{w\text{-}bulk}$), bulk decane ($S_{o\text{-}bulk}$), 100% brine saturated ($S_{w\text{-}100\%}$) and 100% decane ($S_{o\text{-}100\%}$) T_2 distributions to derive the NWI and water saturations as the imbibition process continued. The fitting was done following the procedure outlined above.

Table 1 – Sample Information.

Sample	Length (cm)	Diameter (cm)	Rock Type	Original State	Porosity (%) Helium, MICP	LECO TOC (wt%)	XRD Mineralogy (wt%)
2-P2	5.21	2.58	chalk	100% Brine Saturated	4.3, 4.1	0.39	Quartz: 3.8 Feldspar: 2.3 Carbonate: 85 Total clay: 6.6 Pyrite: 1 Marcasite: 0.7
2-P1A	4.59	2.6	chalk	100% Decane Saturated			
7-P2	4.93	2.61	marl	100% Brine Saturated	12.5, 12	4.38	Quartz: 21.1 Feldspar: 3.9 Carbonate: 46.5 Total clay: 23.4 Pyrite: 4.6 Marcasite: 0.6
7-P3A	4.97	2.55	marl	100% Decane Saturated			

Table 2 – CPMG Parameters.

Sample	Recycle delay (ms)	Signal to Noise Ratio	Tau (µs)	Number of Echoes	NMR Porosity (p.u.) or Volume (ml)	P90 (µs)
2-P2	750	200	50	5000	4.7 p.u.	7.61
2-P1A	750	200	50	5000	4.3 p.u.	7.61
7-P2	3000	200	50	20000	13.7 p.u.	7.61
7-P3A	750	200	50	5000	12.8 p.u.	7.61
Bulk Decane	18750	164	50	125000	4.69 ml	7.61
Bulk Brine	22500	236	50	150000	6.38 ml	7.61

Figure 2: Water droplets seen on the surface of the sample after it was submerged in decane.

Results

Figure 3 shows the T_2 spectra recorded for the 2-P1A/2-P2 twin shale samples. The left-hand panel of Figure 3 shows several distributions recorded as twin 2-P1A (originally 100% decane saturated) imbibed brine. The right-hand panel of Figure 3 shows several distributions recorded as twin 2-P2 (originally 100% brine saturated) imbibed decane. At first glance the T_2 distributions recorded during imibibition seem to be changing more rapidly for sample 2-P1A as compared to sample 2-P2. This was an early indication that these twins are water wet, because the 100% decane saturated sample (2-P1A) is readily imbibing brine while the 100% brine saturated sample (2-P2) is not imbibing decane as quickly.

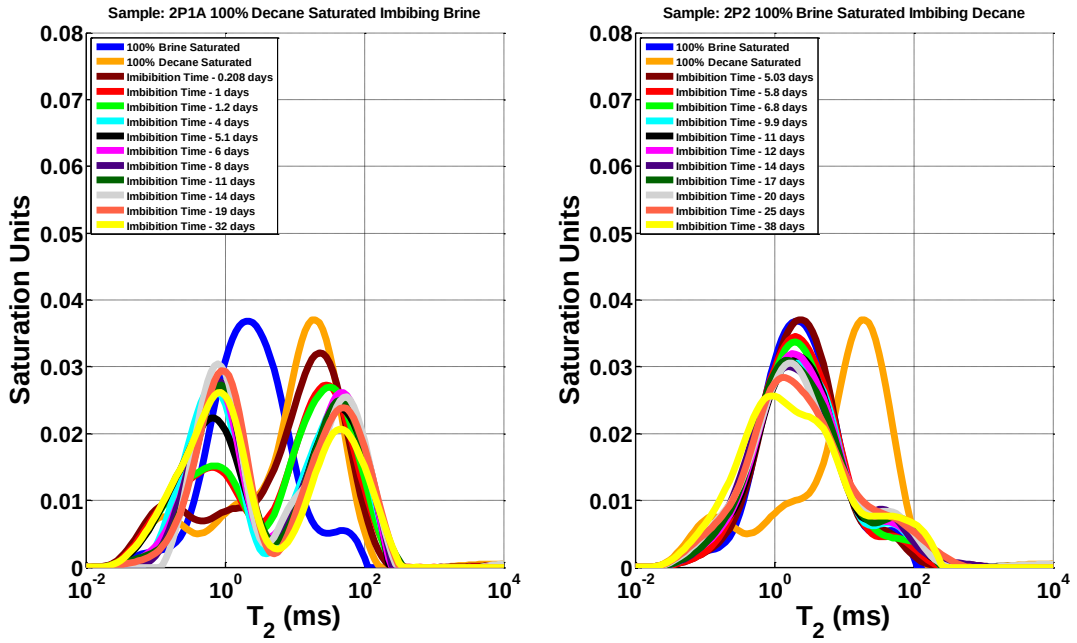

Figure 3: The T_2 spectra recorded for the 2-P1A/2-P2 twin shale samples. The left-hand panel shows several distributions recorded as twin 2-P1A (originally 100% decane saturated) imbibed brine. The right-hand panel of shows several distributions recorded as twin 2-P2 (originally 100% brine saturated) imbibed decane. Also shown are the 100% brine saturated, 100% decane saturated, bulk brine and bulk decane T_2 distributions. This data was employed to derive the wettability and saturation as a function of imibition time.

To confirm this initial analysis and quantify the change in wettability over time, each of the T_2 distributions recorded during the imbibition process for both twins were processed through the wettability fitting routine described earlier. As described, this fitting routine also requires the 100% brine saturated, 100% decane saturated, bulk brine and bulk decane T_2 distributions. These distributions are all also shown in both the left and right panels of Figure 3.

Figure 4 shows the results of the wettability analysis for twins 2-P1A and 2-P2. The left-hand panel displays the wettability as a function of imbibition time for both samples, while the right-hand panel of Figure 4 shows the water saturation as a function of imbibition time for both samples. Looking at the wettability change for twin 2-P1A (Figure 4 – left panel - blue trace), it is observed that the rock started oil wet but changed to water wet within the first 24 hours of brine imbibition. The NMR wettability index then continued to increase for the next three days until it stabilized around 0.90 at about day five. During the first five days of the experiment, the water saturation for twin 2-P1A (Figure 4 – right panel – blue trace) has not been as stable. It started around 30% during day one and dropped to approximately 20% by day five. Clearly it is not physically possible for a decane saturated rock which is imbibing brine to have its water saturation go down. Instead the instability in the data during the first the first five days

reflects active changes ongoing in the rock during this period. These changes lead to instability in the predictions. Since the wettability stabilized at day five, the water saturation has shown a slow increase from approximately 0.2 to 0.3.

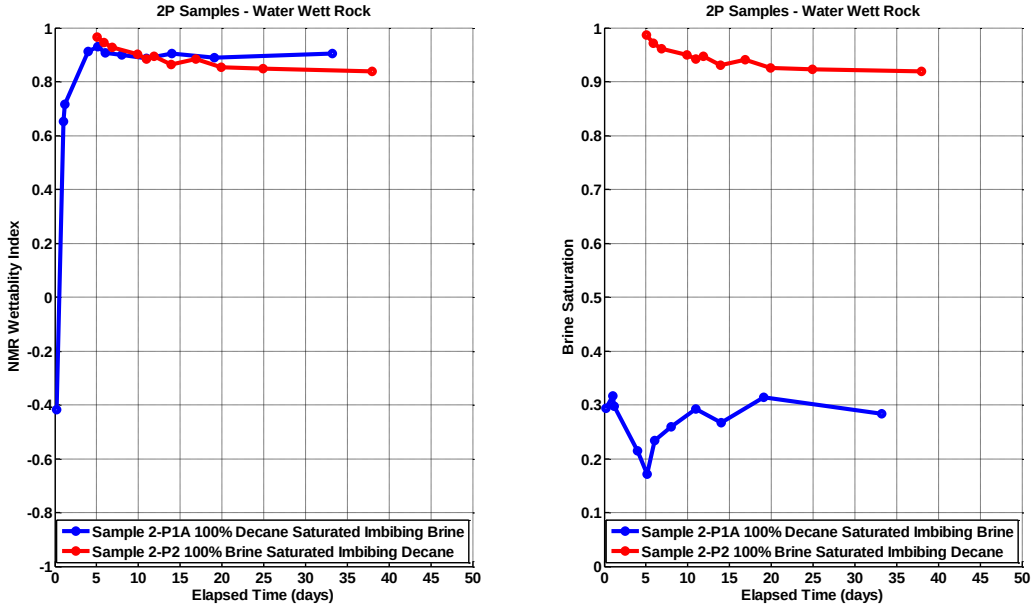

Figure 4: The results of the wettability analysis for twins 2-P1A and 2-P2 are shown. The left-hand panel shows the wettability as a function of imbibition time for both samples, while the right-hand panel shows the water saturation as a function of imbibition time for both samples.

The wettability and saturation levels for sample 2-P2, decane imbibition into brine, have not changed as rapidly as for sample 2-P1A. While there are no measurements during the first five days of decane imbibition, neither the wettability (Figure 4 – left panel – red trace) nor the water saturation (Figure 4 – right panel – red trace) have changed significantly between days five and seventeen. The wettability has only slowly decreased from 0.96 to 0.83 during this time while the water saturation has decreased from 97% to 92% during the same time. What can be said is that the wettability of the two twins have approached one another over time while the saturations remain vastly different.

A similar analysis has also been carried out on twins 7-P3A/7-P2 and Figure 5 shows the T_2 distributions recorded during the imbibition process for each twin. The left-hand panel of Figure 5 shows the distributions recorded as twin 7-P3A (originally 100% decane saturated) imbibed brine. The right-hand panel of Figure 5 shows several distributions recorded as twin 7-P2 (originally 100% brine saturated) imbibed decane. As with the first set of twin shale samples, at first glance the T_2 distributions recorded during imibibition gives an indication as to whether these shales are water wet or oil wet. Sample 7-P2 seem to be imbibing decane more rapidly than sample 7-P3A was imbibing brine indicating that the sample is likely oil wet.

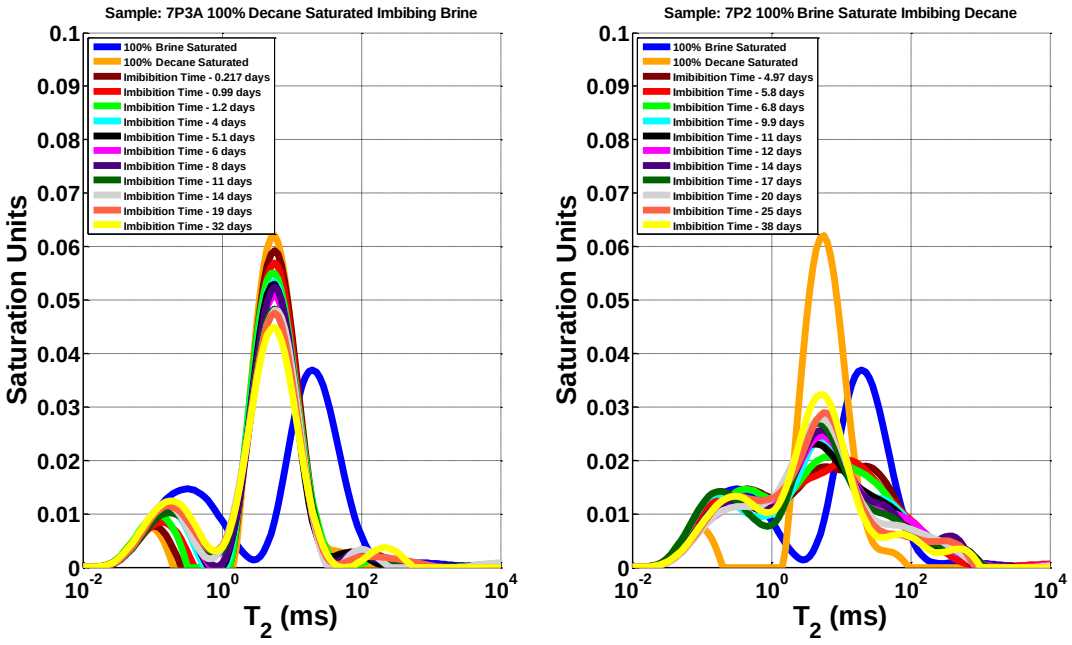

Figure 5: The T_2 spectra recorded for the 7-P3A/7-P2 twin shale samples. The left-hand panel shows several distributions recorded as twin 7-P3A (originally 100% decane saturated) imbibed brine. The right-hand panel of shows several distributions recorded as twin 7-P2 (originally 100% brine saturated) imbibed decane. Also shown are the 100% brine saturated, 100% decane saturated, bulk brine and bulk decane T_2 distributions. This data was employed to derive the wettability and saturation as a function of imbibition time.

To confirm this initial analysis the T_2 distributions recorded during imibibition were processed through the wettability fitting routine. Again the 100% brine saturated, 100% decane saturated, bulk brine and bulk decane T_2 distributions are also employed in the fitting and are included Figure 5.

Figure 6 shows the results of the wettability analysis for twins 7-P3A and 7-P2. The left-hand panel displays the wettability as a function of imbibition time for both samples, while the right-hand panel shows the water saturation as a function of imbibition time for both samples. The wettability change for twin 7-P3A (Figure 6 – left panel - blue trace) shows that the NWI started around -0.7 and has slowly increased to around -0.4 over the thirty days of the 100% decane saturated sample imbibing brine. During this same time period, the water saturation for twin 7-P3A (Figure 6 – right panel – blue trace) has also slowly increased from approximately 15% to around 30% by day thirty. The wettability and saturation levels have changed more rapidly for sample 7-P2 as compared to sample 7-P3A. Unfortunately, there are no measurements during the first five days of decane imbibition. However, since the fifth day the wettability (Figure 4 – left panel – red trace) and the water saturation (Figure 4 – right panel – red trace) have changed significantly. The NWI has decreased steadily from ~0.05 to -0.30 during this time while the water saturation has remained relatively constant (~35%) during the same time. As with the first set of twins, the wettability for these samples also seem to be approaching one another as the imbibition time increases.

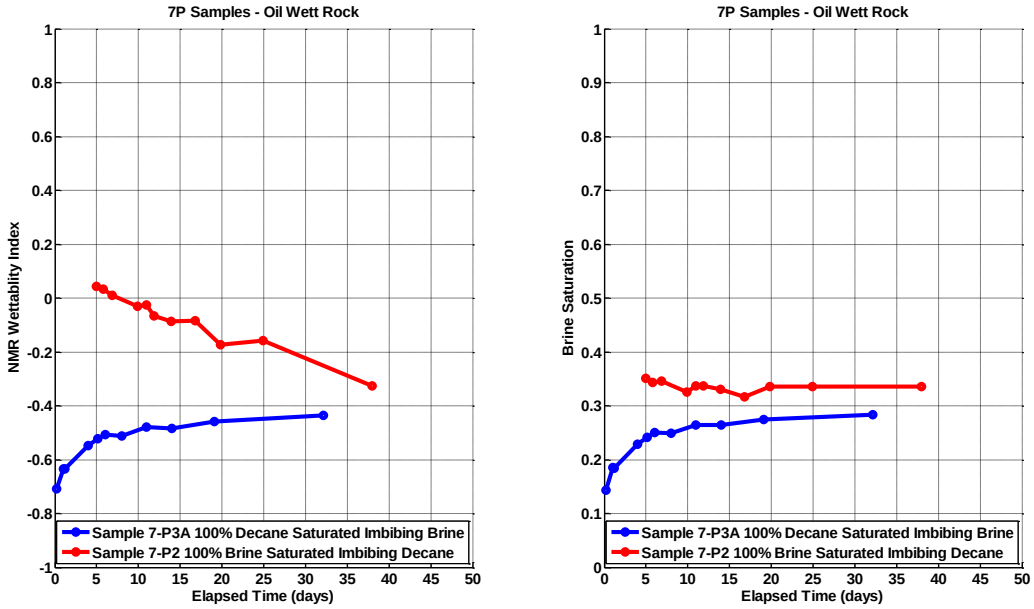

Figure 6: The results of the wettability analysis for twins 7-P3A and 7-P2 are shown. The left-hand panel shows the wettability as a function of imbibition time for both samples, while the right-hand panel shows the water saturation as a function of imbibition time for both samples.

Discussion

From the results section, it is clear that T_2 distributions are changing as a function of saturation change in the samples. This information is used with the bulk T_2 distributions of decane and brine to generate NWI values for the samples. The samples display a dynamic wettability index that slowly asymptotes towards equilibrium as imbibition proceeds. It is expected that wettability state will change with saturation, as changes in the distribution of fluid-solid contacts will render differences in NMR relaxation of the fluid molecules in direct contact with those varied surfaces. Despite significantly lower porosity than sample 7-P3A (see Table 1), sample 2-P1A, a chalk, imbibes water more successfully than sample 7-P3A, an organic-rich marl; correspondingly, the NWI for the chalk sample is very high, > 0.8, indicating strongly water wet. The majority of brine imbibition in the chalk occurred very quickly, within 24 hours, and the chalk did not readily imbibe decane, remaining highly water wet in terms of NWI. Meanwhile, sample 7-P2 imbibed decane only slightly more rapidly than sample 7-P3A imbibed brine, indicating that the sample is slightly oil wet. leaning towards mixed wet; correspondingly, the NWI for these sample is within the bounds of -0.4 to 0.2 for the duration of the experiment.

While there were not conventional wettability measurements (i.e., Amott and USBM methods) available for comparison on these samples, the NWI findings agree with previous spontaneous imbibition studies performed by the operator on plugs from the same reservoir as the plugs used in this study. Those tests revealed that counter-current imbibition was an actuation mechanism for mobilizing oil and that this effect steadied out within only a few days for both marl and chalk plugs. However, the chalk samples were found to release (?) oil more efficiently due to their water-wet preference. Hence, despite higher porosity and, therefore, higher bulk volume hydrocarbon (BVH) in marl facies, chalk facies with decent porosity may contribute more meaningful to production in the studied reservoir due to wettability-driven deliverability. This hypothesis requires more testing but wettability controls could potentially steer landing zones and completions fluid design during development of similar fields. Note that, though

subtle, changes in the measured NWI and saturation due to imbibition in the tests performed in this study persisted well beyond a few days, indicating continued long-term fluid percolation through the matrix.

Wettability is also a key driver in water block mechanisms due to capillary end effects, a type of formation damage due to a capillary discontinuity of the wetting phase at the matrix-fracture interface [10] [11]. The capillary end effect in water wet rocks would cause an increase in water situation near the matrix-fracture interface, blocking the efficacy of hydrocarbon production, especially gas. Ergo, wettability characterization is prudent in unconventional reservoirs, where production is enabled by increased fracture surface area.

Finally, the NWI approach allows oil/brine saturations to be determined without the aid of any special oil or brine, such as D2O. This advantage enables the utilization of NMR measurements to nondestructively monitor changes in wettability in real time (i.e. during a flooding experiment or an aging procedure). As opposed to Amott and USBM methods, there is no need to do forced imbibition which can be challenging in low permeability unconventional samples.

Conclusions

The NWI as presented here worked well on the tested unconventional samples for quantifying changes in sample wettability over time, establishing the potential of the methodology as a viable diagnostic SCAL option for reservoir characterization. Naturally, continued verification against various unconventional rock types will enable further determination of the robustness of the methodology.

The results confirm the hypothesis of the wettability of the unconventional rock types investigated: for initial testing, twins of tight samples from the same depths were utilized; these samples were selected based on end-member responses to complementary routine core analysis parameters. In each twin set, one sample was 100% saturated with brine, and another was 100% saturated with oil. NMR T_2 spectra of the 100% brine saturated and 100% oil saturated plugs were obtained. Time-lapse NMR measurements during spontaneous imbibition enabled monitoring of sample saturation changes with time. Using these data, along with the T_2 spectra of bulk oil and brine, the NWI for the mixed saturation sample was calculated. The NWI was then compared to contextual knowledge about the reservoir's production, as well as other complementary routine and special core analysis data, enabling an assessment of the value of the NWI method for tight rocks.

References

1. Fleury, M. and Deflandre, F., "Quantitative evaluation of porous media wettability using NMR relaxometry", Magnetic Resonance Imaging (2003), **21**, 385-387.
2. Howard, J.J., "Quantitative estimates of porous media wettability from proton NMR measurements", Magnetic Resonance Imaging (1998), **16**, 529-533.
3. Borgia, G. C., Fantazzini, P. and Mesini, E., "Wettability effects on oil-water configurations in porous media, a nuclear magnetic resonance relaxation study", J. Appl. Phys., **70**, 7623-7625.
4. Hsu, W. F. and Flumerfelt, R. W., "Wettability of porous media by NMR relaxation methods", SPE Annual Technical Conference and Exhibition, Washington, D.C., USA, 4-7 October 1992.
5. Freedman, R., Heaton, N., Flaum, M., Hirasaki, G. J., Flaum, C. and Hurlimann, M., "Wettability, saturation and viscosity from NMR measurements", SPEJ, **8**, 317-327.

6. Looyestijn, W.J. and Hofman, J.P., “Wettability Index Determination by Nuclear Magnetic Resonance”, SPE 93624, presented at the MEOS, Bahrain, March 2005. Published in SPEREE April 2006, pp 146 – 153.
7. Looyestijn, W., Zhang, X., and Hebing, A., "How can NMR assess the wettability of a chalk reservoir", Society of Core Analysts, Vienna, Austria, 27 August-1 September 2017.
8. GIT Systems and LithoMetrix User Manual, Revision 1.9, Green Imaging Technologies.
9. Geo-Spec 2-75 User Manual, Version 1.8, Oxford Instruments.
10. Huang, D.D. and Honarpour, M.M., “Capillary end effects in coreflood calculations”, Journal of Petroleum Science and Engineering (1998), **19**, 102-117.
11. Elputranto, R. and Akkutlu, I.Y., “Near Fracture Capillary End Effect on Shale Gas and Water Production”, URTeC, Houston, TX, USA, 23-25 July 2018, DOI:10.15530/urtec-2018-2902627.